CARBON 60 (2013) 246–253

Available at www.sciencedirect.com

SciVerse ScienceDirect

journal homepage: www.elsevier.com/locate/carbon

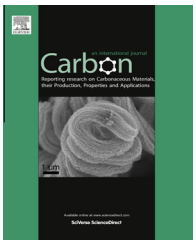

In situ transmission electron microscope tensile testing reveals structure–property relationships in carbon nanofibers

Allison M. Beese [a], *Dimitry Papkov* [b], *Shuyou Li* [c], *Yuris Dzenis* [b,*], *Horacio D. Espinosa* [a,*]

[a] *Department of Mechanical Engineering, Northwestern University, 2145 Sheridan Rd., Evanston, IL 60208, USA*
[b] *Department of Mechanical and Materials Engineering, University of Nebraska-Lincoln, W315 Nebraska Hall, Lincoln, NE 68588, USA*
[c] *Northwestern University Atomic and Nanoscale Characterization Experimental Center, 2220 Campus Drive #2036, Evanston, IL 60208, USA*

ARTICLE INFO

Article history:
Received 22 February 2013
Accepted 6 April 2013
Available online 16 April 2013

ABSTRACT

Tensile tests were performed on carbon nanofibers *in situ* a transmission electron microscope (TEM) using a microelectromechanical system (MEMS) tensile testing device. The carbon nanofibers tested in this study were produced via the electrospinning of polyacrylonitrile (PAN) into fibers, which are subsequently stabilized in an oxygen environment at 270 °C and carbonized in nitrogen at 800 °C. To investigate the relationship between the fiber molecular structure, diameter, and mechanical properties, nanofibers with diameters ranging from ~100 to 300 nm were mounted onto a MEMS device using nanomanipulation inside the chamber of a Scanning Electron Microscope, and subsequently tested in tension *in situ* a TEM. The results show the dependence of strength and modulus on diameter, with a maximum modulus of 262 GPa and strength of 7.3 GPa measured for a 108 nm diameter fiber. In particular, through TEM evaluation of the structure of each individual nanofiber immediately prior to testing, we elucidate a dependence of mechanical properties on the molecular orientation of the graphitic structure: the strength and stiffness of the fibers increases with a higher degree of orientation of the 002 graphitic planes along the fiber axis, which coincides with decreasing fiber diameter.

1. Introduction

Carbon nanofibers, which have high strength and stiffness, as well as unique thermal and electrical properties, have numerous applications in a wide range of fields, including: use in structural applications as reinforcement agents in composite materials, use in protective textiles, use in environmental applications as filtration membranes, use in electronics, use in hydrogen storage applications, use in lithium ion batteries, and use in medical applications as wound dressings [1–8]. In many of these applications, the mechanical integrity of the carbon nanofibers is paramount, thus it is critical to characterize the mechanical behavior of individual nanofibers.

The primary precursors used for large-scale production of carbon nanofibers, where the mechanical integrity of the fibers is important, are polyacrylonitrile (PAN), rayon, and pitches [9]. As discussed in a recent comprehensive review of PAN-based nanofibers, the most promising technique for synthesis of carbon nanofibers is electrospinning, with PAN being the most frequently used polymer precursor [1].

PAN-derived carbon fibers are produced by electrospinning, followed by stabilization and carbonization of the resulting fibers [1,10–13]. Electrospinning allows for the production of fibers with diameters between 10 nm and 10 μm [14,15]. One benefit of carbon fibers with diameters on the order of 100 nm compared to fibers with 10 μm in diameter is

* *Corresponding authors.*
E-mail addresses: ydzenis@unl.edu (Y. Dzenis), espinosa@northwestern.edu (H.D.Espinosa).
0008-6223/$ - see front matter
http://dx.doi.org/10.1016/j.carbon.2013.04.018

the significantly larger surface area to volume ratio of the nanofibers, which can reach 10^2 times that of the microfibers [16]. The thinner fibers are thus attractive for use in composites, where mechanical integrity between the matrix and the surface of the reinforcing agent is critical for effective load transfer [2,17]. In addition, the thinner fibers require significantly less carbonization time, resulting in lower manufacturing costs than those of larger fibers [18].

To quantify the mechanical properties of carbon nanofibers, researchers have applied a variety of methods, including: using an atomic force microscope (AFM) to indent individual fibers [19], performing tests on yarns composed of tens to hundreds of carbon nanofibers to obtain mechanical yarn properties that are a function of both the mechanical properties of the individual fibers and the structural arrangement of the fibers within the yarn [18], performing tensile tests on sheets of nanofibers to obtain average mechanical properties of the individual fibers collectively [20], and measuring the bending modulus using resonant frequency experiments in the chamber of a scanning electron microscope (SEM) and subsequently using an AFM cantilever as a load sensor during SEM imaging to measure the strength of the fiber [21]. A recent review highlights the lack of data on individual carbon nanofibers due in large part to the challenges present in isolating, manipulating, and gripping individual fibers [1]. Tensile tests of individual carbon fibers have been successfully performed by Arshad et al. [17] using a microelectromechanical system (MEMS) based device to load individual samples *in situ* a SEM.

In particular, Arshad et al. [17] performed a study on the effect of stabilization and carbonization parameters on resulting carbon fiber properties. They characterize the structure of the resulting fibers using macroscale procedures, and through SEM studies, quantify the mechanical properties of individual fibers with diameters ranging from 200 to 500 nm for carbonization temperatures ranging from 800 to 1700 °C.

Here, we present an experimental study in which we use a MEMS device to apply tensile loads to individual carbon nanofibers *in situ* a transmission electron microscope (TEM). This allows both characterization of the structure of a nanofiber and measurement of its mechanical properties, in order to identify structure–property relationships in electrospun carbon nanofibers. The Espinosa group has successfully employed this technique in nanomechanics studies of CNTs [22], ZnO nanowires [23,24], GaN nanowires [25], and Ag nanowires [26]. The data reported in the present study augment those previously reported [17] by providing data for smaller diameter samples, in addition to the powerful *in situ* TEM classification of the molecular arrangement of the individual nanofibers being tested.

2. Materials and methods

2.1. Materials

The fibers used were fabricated by the Dzenis group through processing similar to the one reported in [27]. We note that the samples were produced by co-spinning double wall nanotube (DWNT) bundles (MER Corp.) and PAN polymer (Pfaltz and Bauer, Inc.; cat# P21470, MW 150,000). However, based on high resolution TEM imaging, we note that the samples individually selected for nanoscale mechanical tests contained no DWNTs inside, nor any evidence that their structure was at all affected by the presence of DWNT elsewhere in the macroscopic mat of carbon nanofibers. Thus, the fibers tested in this study are carbonized PAN fibers.

The DWNTs were dispersed in dimethylformamide (DMF) and were subjected to high speed shear mixing at 17,500 rpm for 6 h. The PAN polymer was added to the mixture and fully dissolved to produce a 10% PAN/0.12% DWNT wt/wt dispersion in DMF. The dispersion was then ultrasonicated in a bath for 1.5 h. The starting weight ratio resulted in a 1.2% weight fraction of DWNTs in the PAN nanofibers after electrospinning, none of which were present in the tested nanofibers. Nanofibers were fabricated using electrospinning at 12 kV with a 0.6 ml/h feed rate, a 20 ga needle, and a spinneret-collector distance of 20 cm.

The as-produced nanofibers were subsequently converted to carbon nanofibers following an established procedure of stabilization followed by carbonization [10–12]: first, mats of nanofibers were stabilized in an oxygen atmosphere at 270 °C for 1 h, and second, carbonization was performed at 800 °C in nitrogen, at a heating rate of 10 °C/min and dwell time of 1 h.

2.2. *In situ* TEM mechanical testing

Electrospun carbon nanofibers, with diameters ranging from ~100 to ~300 nm, and a gauge length of ~2.5 μm, were tested in tension on a MEMS device *in situ* a TEM by the Espinosa group, and stress versus strain data were obtained. The MEMS testing stage used is comprised of four main components: a thermal actuator, a load sensor, and two opposing shuttles, one connected to the thermal actuator and the other to the load sensor (Fig. 1) [28–31]. For a tensile test, a sample is gripped to each of the two opposing shuttles, and increasing currents are applied to the thermal actuator, which provides a tensile displacement to one end of the sample. The force through the sample causes a displacement of the folded beams of the load sensor; thus, the force can be calculated by multiplying the stiffness of the load sensor by the deflection of the load sensor. For a review of the *in situ* TEM experiments using MEMS technology, see [32].

Through the electrospinning and carbonization processes described above, the samples were prepared as a mat of carbonized nanofibers. To extract samples from the mat for testing, an exfoliation process was performed [33], whereby nanofibers were transferred to a TEM grid. Straight samples with a uniform diameter were selected for testing. Each sample was transferred to a MEMS testing device through use of a nanomanipulator (Klocke) inside the chamber of an SEM (FEI NovaSEM 800). The sample was placed to span the gap between the two shuttles. Each end of the sample was fixed to one of the two shuttles using electron beam induced deposition (EBID) of a local carbonaceous platinum rectangular spot 'weld' approximately 250 nm long along the axial direction of the fiber, and 500 nm wide perpendicular of the fiber axis (see [25]). These welds, applied away from the gauge region,

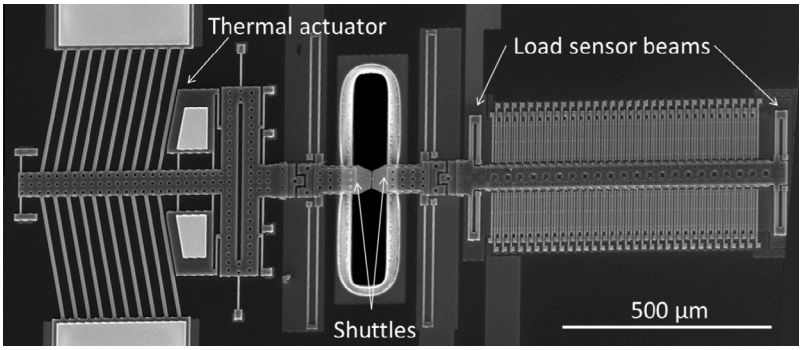

Fig. 1 – MEMS device used for *in situ* TEM mechanical testing. An electrical current sent through the thermal actuator causes the chevron beams to expand, moving the left shuttle to the left. The sample is clamped to the left and right shuttles with EBID platinum, and the force through the sample is measured by the deflection of the folded load sensor beams on the right.

served to grip the sample to the shuttles during tensile loading.

Once a sample was mounted onto a MEMS device, the device was loaded into a high resolution JEOL 2100F field emission TEM. Prior to tensile testing, selected area electron diffraction (SAED) was performed along the length of each mounted nanofiber. Of particular interest is the spread of the 002 graphitic crystal diffraction pattern. A diffuse pattern, with equal signal intensity around the entire 002 diffraction ring would indicate a random orientation of the 002 crystal planes in the fiber, whereas discrete points would indicate perfect alignment of the crystal direction along a specific fiber direction. Therefore, these patterns were analyzed for each sample to characterize the degree of molecular orientation of the graphitic crystalline planes in the carbonized fiber.

Tensile tests were performed in the TEM at 200 keV. A stepwise displacement is applied to the nanofibers by increasing the current through the thermal actuator of the MEMS device in discrete steps [28–31]. Digital Image Correlation (Vic2D, Correlated Solutions) was used to quantify the displacements between shuttles during the test, and immediately after the test for calibration purposes. The load was measured by multiplying the calibrated MEMS device load sensor stiffness (1623 N/m) [30] by the difference in thermal actuator displacement and the displacement measured during each testing step. The displacement of the thermal actuator as a function of current was calibrated after each test, by unloading the thermal actuator with the same currents applied during the loading process. Thus, the distance between shuttles as a function of applied current, but with zero applied force (and therefore a stationary load sensor) was measured.

3. Results and discussion

There are several advantages of testing fibers using MEMS *in situ* a TEM. In terms of measuring mechanical properties, one significant advantage is that the diameter of the sample to be tested can be explicitly and precisely measured along the entire gauge length before testing. This is particularly important for electrospun fibers, which typically contain beads, or local regions of larger diameter, along the length of the fiber, which would not be detected in a sample without SEM or TEM imaging [16]. Thus, the imaging of fiber samples in the SEM and TEM allows for an accurate calculation of the cross-sectional area, and as a result, stress and modulus measurements. Also, the selection of a constant diameter fiber allows for the accurate measurement of the inherent mechanical properties not affected by local bead defects or changes in diameter. In addition, using the MEMS device, displacements of ~2 nm may be applied to the 2.5 μm gauge length sample, resulting in strain resolution measurements on the order of 0.1%, allowing for an accurate modulus measurement of these stiff and brittle samples. Finally, performing the test *in situ* a TEM allows for direct evaluation of the molecular structure prior to testing, providing a powerful technique through which structure–property relationships can be directly studied.

In situ TEM tensile tests were performed on five carbon nanofibers, covering a range of diameters from ~100 to 300 nm. Fig. 2a provides successive images of applying an increasing tensile displacement to a nanofiber up to failure, with a high resolution image of the failure surfaces in Fig. 2b. Note that due to difficulties in nanomanipulation within a SEM chamber with only four degrees of freedom, and the tendency for nanosamples to snap to the shuttles when in close proximity, perfect alignment of the nanofibers with the tensile axis of the shuttles is not possible. Therefore, only nanofibers with a tensile axis less than 15° from the MEMS tensile direction were considered, and any misalignment is taken into account when computing the stress and strain. Also note that while the EBID platinum deposition is applied locally as spot welds to the ends of the sample for gripping purposes, a very small amount may diffuse onto the specimen gauge region. In addition, imaging of the sample in SEM and TEM can lead to a very thin layer of amorphous carbon coating the sample. Only samples with minimal platinum coating were considered. Taking into account that this coating material, if continuous along the length of the nanofibers, can contribute to the measured properties, we calculate the maximum error on the modulus measurements. In particular, following the detailed analysis presented in [26], which showed that the modulus of this coating, if assumed to be continuous, is ~13 GPa, we calculate an error in the modulus measurement of 5% or less in all of the tests reported here.

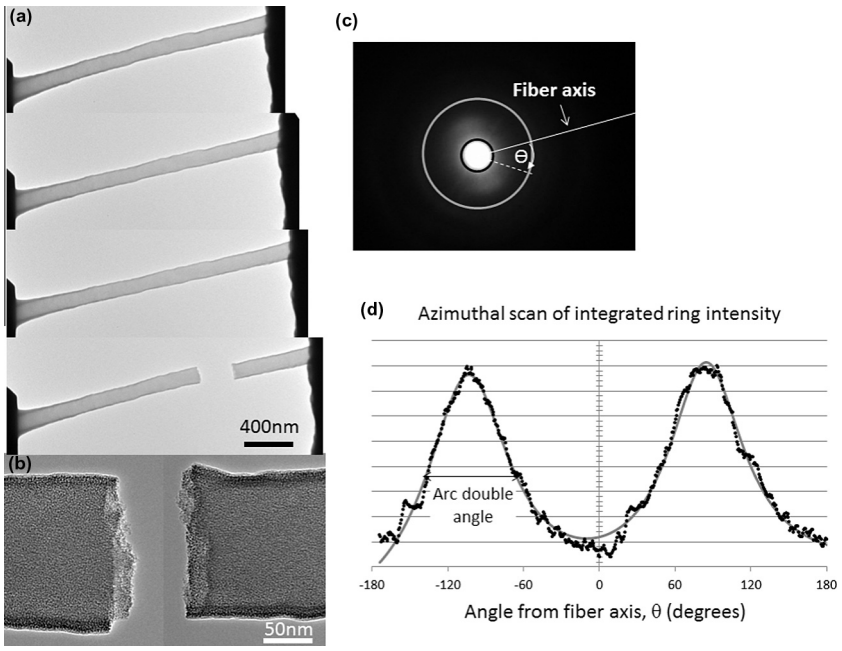

Fig. 2 – (a) Sequential TEM images during a tensile test. (b) High resolution image of the fracture surface in (a). (c) Example SAED pattern with fiber axis direction indicated, along with the angle from the fiber axis, θ. A schematic overlay of white and black circles indicates the ring of 002 graphitic plane signal. (d) Integrated intensity of the 002 signal ring of the SAED pattern in (b) as a function of the angle from the fiber axis (data points represented by solid symbols with solid line indicating best fit line), with the full width at half maximum, or arc double angle, indicated.

As a means of evaluating and comparing the nanofibers structures among samples, SAED is performed along the length of each nanofibers prior to testing. Fig. 2c shows an SAED pattern for the ~100 nm diameter nanofiber. The 002 graphitic plane diffraction pattern is contained in the ring between the white and black circles schematically overlaid on the image. Using QPCED2 [34], the integrated intensity of the ring as a function of angle from the fiber axis is calculated and plotted as shown in Fig. 2d. This integrated intensity versus angle is then fitted with a sinusoidal curve, and the full width at the half maximum (FWHM) of each curve is calculated. The FWHM value corresponds to the double angle of the 002 arc, with larger values indicating more random orientation of the 002 crystal planes, and smaller numbers indicating an increased degree of preferred orientation along the fiber axis. The double arc angle is measured for each of the nanofibers prior to testing, and it generally decreases with decreasing diameter, indicating that as the fiber diameter decreases, the molecular orientation increases (Fig. 3). We note that the comparison of absolute FWHM values between different TEMs with different experimental conditions is not possible. Thus, we use the quantitative calculation of this value to provide understanding of the structure–property relationships in carbon nanofibers tested in the same TEM, under the same experimental conditions. For calculation of FWHM, the average FWHM is taken for the two peaks in each SAED pattern, and in addition, several SAED measurements are taken along the length of each fiber, and the average FWHM values for all of these patterns is taken as the 002 double angle for that fiber.

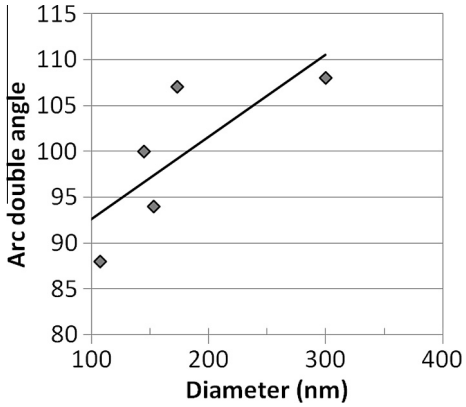

Fig. 3 – Arc double angle of 002 diffraction pattern as a function of diameter (symbols), with a linear best fit line indicating trend.

A stress–strain curve for a 153 nm diameter nanofiber is given in Fig. 4, where it is shown that the fibers deform approximately linearly elastically until failure. The maximum stress and modulus measured for each of the samples, as a function of nanofiber diameter, is reported in Fig. 5. The modulus is measured in a region of the data where its accuracy is the highest. It is instructive to compare the results obtained in this study with those obtained in a similar study, where carbonized PAN fibers were tested using microfabricated devices [17]. In particular, we compare the modulus and strength measurements from that study for samples carbonized at 800 °C, the same temperature used in the present study. We note that while the previous study showed a

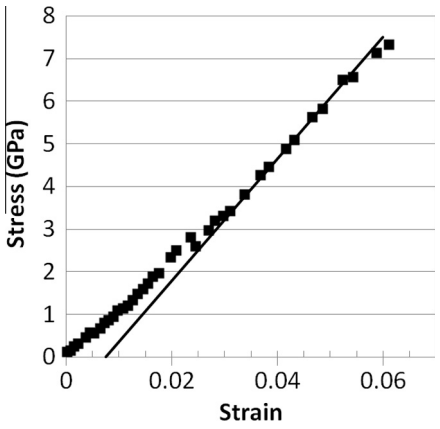

Fig. 4 – Engineering stress-strain curve (solid squares) for 153 nm diameter carbonized fiber, with measured elastic modulus shown as a solid line.

very slight increase in stress and modulus with decreasing diameter, the results presented here augment the previous data, by revealing the trends for smaller diameter fibers that were not previously tested, while also showing agreement with the previously obtained data at larger diameters. In particular, we measured maximum stresses 2.8 times higher than the highest previously reported for a carbonization temperature of 800 °C as we tested fibers below 200 nm in diameter. It appears that the maximum stress saturates at diameters below 150 nm, suggesting that at that diameter, we are probing the materials intrinsic properties. This observation requires further investigation at diameters below 100 nm, which in general are difficult to manufacture. The modulus measured increases with decreasing diameter, again complementary to the data reported by Arshad et al. [17]. The maximum modulus we measure is 2.3 times higher than that reported in the previous study. We also note that the strengths reported here for nanofibers carbonized at 800 °C with diameters of 153 nm and below, exceed those of all nanofibers reported in [17], including those carbonized at 1100–1700 °C. Also, the modulus measured for the 108 nm diameter fiber in the present study exceeds all moduli measured in the previous study except one, where the fiber was carbonized at 1700 °C (fiber diameter of ~150 nm, modulus of ~330 GPa).

The dependence of fiber strength on diameter has been studied in various fibers, and it has been shown that a decreasing diameter, resulting in smaller fiber volume, also results in a decreased number of initial defects or cracks in a material, and thus a decreased probability of failure in brittle materials (e.g., [35,36]). In addition to the ability to test smaller diameter nanofibers than the previous study, we are also able to evaluate the molecular properties of each sample tested through SAED inside the TEM. Therefore, to probe the structure–property relationships, we report the mechanical properties measured for each sample as a function of its measured 002 double arc angle (Fig. 6). We note that the strength increases with decreasing double arc angle, or increasing molecular orientation of the graphitic planes along the fiber tensile axis. The strength appears to saturate around 7.3 GPa. In addition, the modulus increases with decreasing double arc angle. Thus, a decrease in diameter results in an increase in the molecular orientation of the 002 graphitic planes along the fiber axis, which in turn manifests into increased mechanical properties of the fiber, namely strength and stiffness. In addition, as noted in [17], carbonization of thinner nanofibers results in a more effective removal of non-carbon elements from the fibers; thus the thinner nanofibers may be more purely carbon.

The fibers presented in this study are envisioned to share similar applications as commercially available carbon fibers, for example, in composites, textiles, or armor. Regarding composite applications, the high surface area to volume ratio inherent to the nanofibers presented in this study provides a higher potential for adhesion to matrix materials than their micrometer diameter counterparts, which is beneficial for increased composite performance.

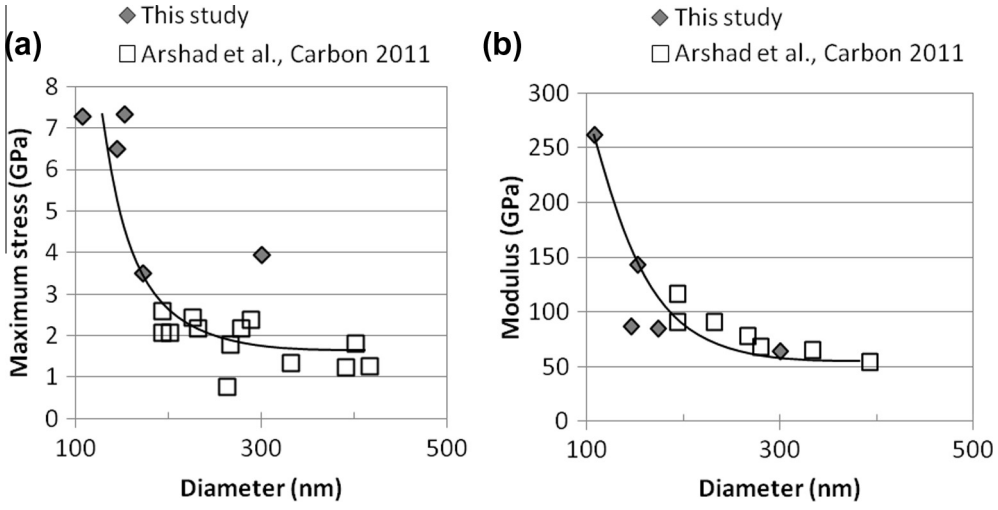

Fig. 5 – Stress (a) and modulus (b) versus carbon nanofibers diameter measured in this study (solid diamonds) compared with data from Arshad et al. [17] (open squares), with the same carbonization temperature. Solid black curves are a guide for the eye to show the mechanical property trends with diameter.

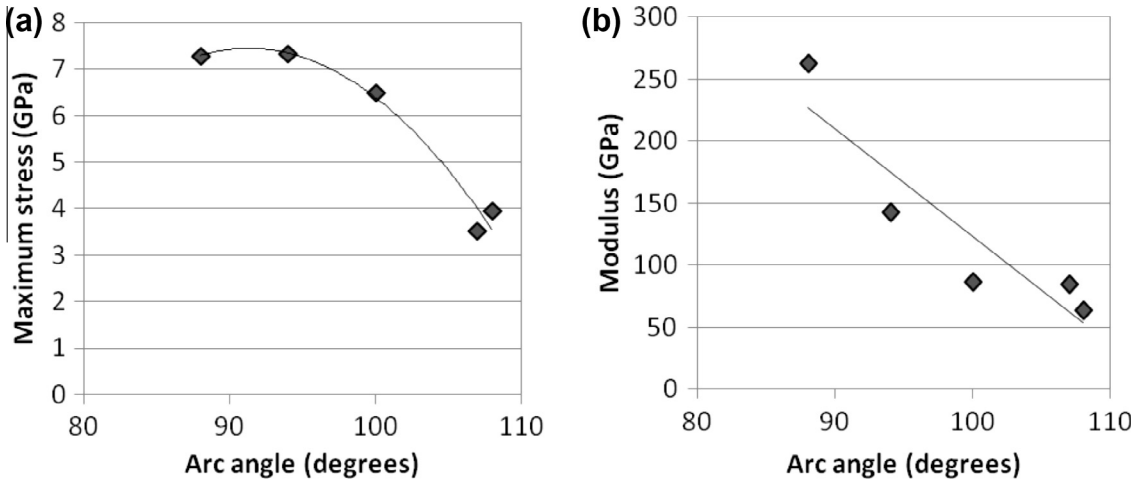

Fig. 6 – Maximum stress (a) and modulus (b) versus 002 double arc angle of fiber, with trends indicated with solid black lines.

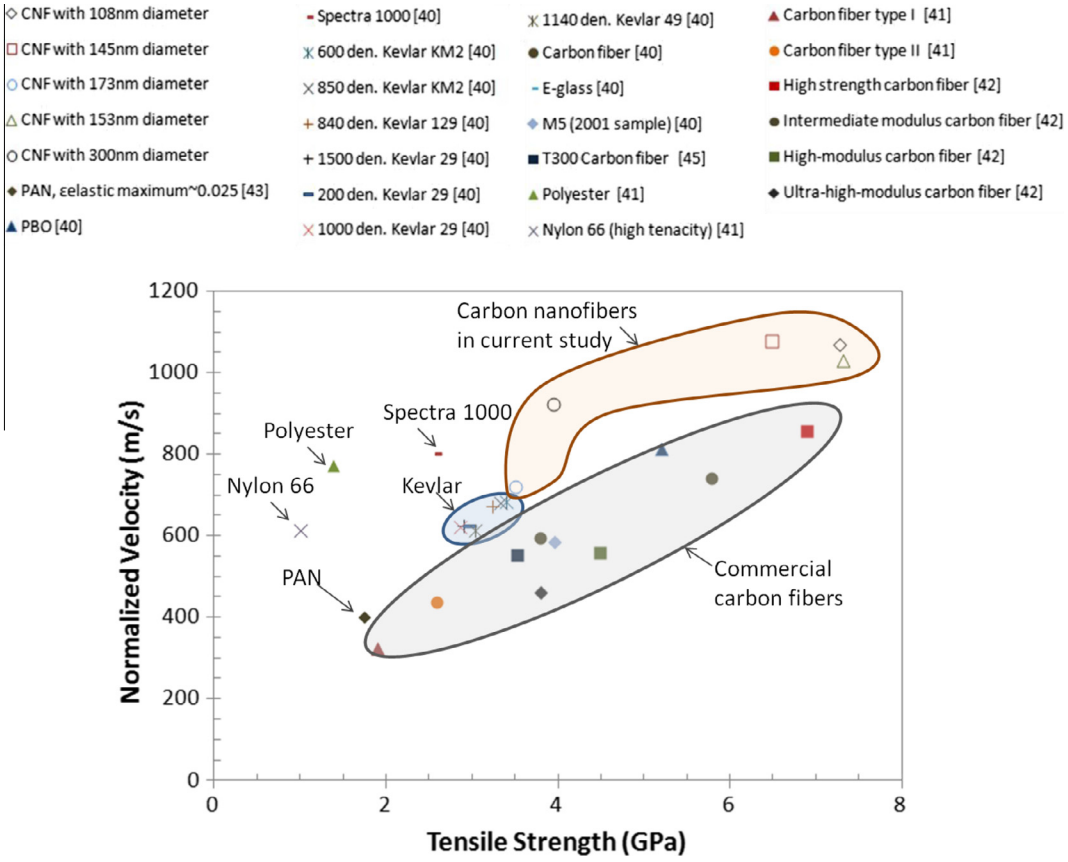

Fig. 7 – Normalized velocity versus tensile strength for commercial fibers compared with the carbon nanofibers presented in the current study.

Regarding fiber effectiveness in armor, Cunniff [37] pointed out that the critical features for fibers used in ballistic applications include: high tensile and compressive moduli, high tensile and compressive strength, high damage tolerance, low specific weight, good adhesion to matrix materials, and good temperature resistance.

To determine the critical mechanical properties relevant to ballistic performance of fibers, Cunniff [37] performed a dimensional analysis utilizing mechanical properties of numerous fibers. He demonstrated that for linear elastic fibers, a qualitative indication of fiber potential effectiveness in ballistic applications is given by:

$$(U^*)^{1/3} = \left(\frac{\sigma\varepsilon}{2\rho}\sqrt{\frac{E}{\rho}}\right)^{1/3}$$

where E is the fiber tensile elastic modulus, ε is the fiber ultimate tensile strain, ρ is the fiber density, and σ is the fiber ultimate axial tensile stress. Thus, the parameter $(U^*)^{1/3}$ is a product of the fiber specific toughness and the strain wave velocity in the fiber for linear elastic fibers.

In particular, this dimensional analysis showed that the $(U^*)^{1/3}$ value of a fiber scales with the V50 velocity of an armor system made from those fibers, where V50 velocity is the velocity at which impacting projectiles defeat a system 50% of the time. Thus, increasing values of $(U^*)^{1/3}$ correspond to increasing V50, and increased protection against projectiles [37].

Phoenix and Porwal [38] performed additional theoretical analysis on ballistic performance, and concluded that the above parameter, which they termed a "normalized velocity parameter," indeed is indicative of the effectiveness of fibers in armor applications, as increased normalized velocity corresponds to increased resistance to ballistic impact.

A detailed review of testing and modeling of ballistic performance of fibers is provided by Tabiei and Nilakantan [39], where they note that while much work has been done on modeling of ballistic performance of fibers woven into fabrics, this topic is very complex, and no single model or parameter can yet describe in a predictive manner the behavior of all of the interrelated variables involved in ballistic effectiveness. Nevertheless, they point out that the normalized velocity parameter first described by Cunniff provides some qualitative insight into the potential functionality of fibers in ballistic applications.

Thus, we compare the normalized velocity parameter, $(U^*)^{1/3}$, determined for the fibers reported in this study with those for commercially available armor fibers in [40–43][1] (see Table S1 in Supporting Information). In addition, Fig. 7 shows the normalized velocity versus tensile strength for the same fibers. This demonstrates the paramount importance of a combination of high stiffness and strength, which is achieved in the carbonized nanofibers measured in the current study. This data points to the potential application of the present carbon nanofibers in armor materials.

4. Conclusions

In summary, we report a study in which we perform *in situ* TEM tensile tests of carbon nanofibers to elucidate the structure-property relationships present in these materials. As we were successful in testing smaller diameter fibers than previously reported, we were able to reveal a dramatic size effect previously not reported, whereby modulus and strength increase significantly in fibers with diameters below 170 nm. In particular, we compare the present results with those reported by Arshad et al. [17], in which electrospun fibers, carbonized at 800 °C were mechanically tested. The comparison shows that the present mechanical data for fibers between 170 and 300 nm agree well with those previously reported for a carbonization temperature of 800 °C; however, the ability to test even smaller diameters in the current study (below 170 nm) revealed a strong size-dependence of nanofiber properties.

We also note that the tensile strengths reported here for fibers carbonized at 800 °C exceed those of fibers produced at even higher carbonization temperatures of up to 1700 °C previously reported [17], while the modulus of the 108 nm diameter nanofibers exceeds all moduli reported in [17] except for one 150 nm diameter nanofibers carbonized at 1700 °C. This has important implications on manufacturing costs, as higher carbonization temperatures require higher production expenses. Thus, the ability to produce fibers with superior properties at lower carbonization temperatures is highly desirable. However, we also note that we expect that the strength and stiffness of the small carbon nanofibers tested here will increase with increased carbonization temperature above 800 °C.

Most significantly, by harnessing the power of *in situ* TEM testing, we are able to directly reveal the relationship between nanoscale structure and mechanical properties in individually isolated nanofibers, whereby decreasing diameter increases the orientation of the graphitic structure along the fiber axis, and in turn the mechanical properties of the fibers. This is indirect evidence of an increasing degree of polymer precursor molecular alignment, during electrospinning, as the jet diameter decreases.

Acknowledgments

This work was funded by the support from ARO through MURI award No. W911NF-09–1-0541, for which the authors are grateful. This work made use of the EPIC facility (NUANCE Center –Northwestern University), which has received support from the MRSEC program (NSF DMR-0520513) at the Materials Research Center, Nanoscale Science and Engineering Center (EEC-0118025/003), both programs of the National Science Foundation; the State of Illinois; and Northwestern University. We thank Dr. Alexander Moravsky for helpful discussions.

Appendix A. Supplementary data

Supplementary data associated with this article can be found, in the online version, at http://dx.doi.org/10.1016/j.carbon.2013.04.018.

REFERENCES

[1] Nataraj SK, Yang KS, Aminabhavi TM. Polyacrylonitrile-based nanofibers. A state-of-the-art review. Prog Polym Sci 2012;37(3):487–513.
[2] Chand S. Carbon fibers for composites. J Mater Sci 2000;35(6):1303–13.

[1] http://www.toraycfa.com

[3] Yun KM, Hogan CJ, Matsubayashi Y, Kawabe M, Iskandar F, Okuyama K. Nanoparticle filtration by electrospun polymer fibers. Chem Eng Sci 2007;62(17):4751–9.
[4] Musale DA, Kumar A. Solvent and pH resistance of surface crosslinked chitosan/poly(acrylonitrile) composite nanofiltration membranes. J Appl Polym Sci 2000;77(8):1782–93.
[5] Im JS, Park SJ, Kim TJ, Kim YH, Lee YS. The study of controlling pore size on electrospun carbon nanofibers for hydrogen adsorption. J Colloid Interface Sci 2008;318(1):42–9.
[6] Kim SU, Lee KH. Carbon nanofiber composites for the electrodes of electrochemical capacitors. Chem Phys Lett 2004;400(1–3):253–7.
[7] Yoon SH, Park CW, Yang HJ, Korai Y, Mochida I, Baker RTK, et al. Novel carbon nanofibers of high graphitization as anodic materials for lithium ion secondary batteries. Carbon 2004;42(1):21–32.
[8] Dresselhaus MS, Dresselhaus G, Eklund PC. Science of fullerenes and carbon nanotubes. San Diego: Academic Press; 1996. 965 p.
[9] Ono H, Oya A. Preparation of highly crystalline carbon nanofibers from pitch/polymer blend. Carbon 2006;44(4):682–6.
[10] Song C, Wang T, Qiu Y, Qiu J, Cheng H. Effect of carbonization atmosphere on the structure changes of PAN carbon membranes. J Porous Mater 2009;16(2):197–203.
[11] Bansal RC, Donnet JB. Polymer reactions. Oxford: Pergamon Press; 1990. p. 501–20.
[12] Sazanov YN, Nud'ga LA, Novoselova AV, Ugolkov VL, Fedorova GN, Kulikova EM, et al. Carbonization of polyacrylonitrile composites with nitrogen-containing cellulose derivatives. Russ J Appl Chem 2004;77(4):639–44.
[13] Litvinov IA, Radimov NP, Lukyanova LM, BitGevorgizov YY, Kasatochkin VI. Scanning electron microscope study of the structure of carbonized polyacrylonitrile fibers. Mech Compos Mater 1971(6):1009–10012.
[14] Jayaraman K, Kotaki M, Zhang YZ, Mo XM, Ramakrishna S. Recent advances in polymer nanofibers. J Nanosci Nanotechnol 2004;4(1–2):52–65.
[15] Formhals A. Process and apparatus for preparing artificial threads. U.S. Patent 1975504; 1934.
[16] Huang ZM, Zhang YZ, Kotaki M, Ramakrishna S. A review on polymer nanofibers by electrospinning and their applications in nanocomposites. Compos Sci Technol 2003;63(15):2223–53.
[17] Arshad SN, Naraghi M, Chasiotis I. Strong carbon nanofibers from electrospun polyacrylonitrile. Carbon 2011;49(5):1710–9.
[18] Fennessey SF, Farris RJ. Fabrication of aligned and molecularly oriented electrospun polyacrylonitrile nanofibers and the mechanical behavior of their twisted yams. Polymer 2004;45(12):4217–25.
[19] Ko F, Gogotsi Y, Ali A, Naguib N, Ye HH, Yang GL, et al. Electrospinning of continuous carbon nanotube-filled nanofiber yarns. Adv Mater 2003;15(14):1161–5.
[20] Hou HQ, Ge JJ, Zeng J, Li Q, Reneker DH, Greiner A, et al. Electrospun polyacrylonitrile nanofibers containing a high concentration of well-aligned multiwall carbon nanotubes. Chem Mater 2005;17(5):967–73.
[21] Zussman E, Chen X, Ding W, Calabri L, Dikin DA, Quintana JP, et al. Mechanical and structural characterization of electrospun PAN-derived carbon nanofibers. Carbon 2005;43(10):2175–85.
[22] Peng B, Locascio M, Zapol P, Li S, Mielke SL, Schatz GC, et al. Measurements of near-ultimate strength for multiwalled carbon nanotubes and irradiation-induced crosslinking improvements. Nat Nanotechnol 2008;3(10):626–31.
[23] Agrawal R, Espinosa HD. Giant piezoelectric size effects in zinc oxide and gallium nitride nanowires. A first principles investigation. Nano Lett 2011;11(2):786–90.
[24] Agrawal R, Paci JT, Espinosa HD. Large-scale density functional theory investigation of failure modes in ZnO nanowires. Nano Lett 2010;10(9):3432–8.
[25] Bernal RA, Agrawal R, Peng B, Bertness KA, Sanford NA, Davydov AV, et al. Effect of growth orientation and diameter on the elasticity of GaN nanowires. A combined in situ TEM and atomistic modeling investigation. Nano Lett 2010;11(2):548–55.
[26] Filleter T, Ryu S, Kang K, Yin J, Bernal RA, Sohn K, et al. Nucleation-controlled distributed plasticity in penta-twinned silver nanowires. Small 2012;8(19):2986–93.
[27] Papkov D, Beese AM, Goponenko A, Zou Y, Naraghi M, Espinosa HD, et al. Extraordinary improvement of the graphitic structure of continuous carbon nanofibers templated with double wall carbon nanotubes. ACS Nano 2012;7(1):126–42.
[28] Zhu Y, Espinosa HD. An electromechanical material testing system for in situ electron microscopy and applications. Proc Natl Acad Sci U S A 2005;102(41):14503–8.
[29] Zhu Y, Moldovan N, Espinosa HD. A microelectromechanical load sensor for *in situ* electron and X-ray microscopy tensile testing of nanostructures. Appl Phys Lett 2005;86(1):013506.
[30] Espinosa HD, Zhu Y, Moldovan N. Design and operation of a MEMS-based material testing system for in-situ electron microscopy testing of nanostructures. J Microelectromech Syst 2007;16(5):1219–31.
[31] Zhu Y, Corigliano A, Espinosa HD. A thermal actuator for nanoscale in-situ microscopy testing: design and characterization. J Micromech Microeng 2006;16(2):242–53.
[32] Espinosa HD, Bernal RA, Filleter T. In situ TEM electromechanical testing of nanowires and nanotubes. Small 2012;8(21):3233–52.
[33] Naraghi M, Filleter T, Moravsky A, Locascio M, Loutfy RO, Espinosa HD. A multiscale study of high performance double-walled nanotube-polymer fibers. ACS Nano 2010;4(11):6463–76.
[34] Li XZ. QPCED2.0: a computer program for the processing and quantification of polycrystalline electron diffraction patterns. J Appl Crystallogr 2012;45(4):862–8.
[35] Griffith AA. Phenomena of Rupture and Flow in Solids. Asm Transactions Quarterly 1968; 61(4): 871-&.
[36] Tagawa T, Miyata T. Size effect on tensile strength of carbon fibers. Materials Science and Engineering a-Structural Materials Properties Microstructure and Processing 1997;238(2):336–42.
[37] Cunniff PM. Dimensionless Parameters for optimization of textile-based body armor systems. In: 18th International symposium on ballistics, San Antonio, TX, November 1999.
[38] Phoenix SL, Porwal PK. A new membrane model for the ballistic impact response and V-50 performance of multi-ply fibrous systems. Int J Solids Struct 2003;40(24):6723–65.
[39] Tabiei A, Nilakantan G. Ballistic Impact of Dry Woven Fabric Composites: A Review. Appl Mech Rev 2008;61(1):010801.
[40] Cunniff PM, Auerbach MA. High performance "M5" fiber for ballistics/structural composites. In: Roylance D, editor. Course mechanical behavior of polymers. MT; 2005.
[41] Bunsell AR. The tensile and fatigue behavior of Kevlar-49 (PRD-49) fibre. J Mater Sci 1975;10:1300–13008.
[42] Gregr J. The complete list of commercial carbon fibers. In: 7th International conference – TEXSCI, Liberec, Czech Republic, September 2010.
[43] Papkov D, Zou Y, Andalib MN, Goponenko A, Cheng SZD, Dzenis YA. Simultaneously strong and tough ultrafine continuous nanofibers. MACS Nano 2013;7(4):3324–31.